Original Article
Yonsei Med J 2022 Apr;63(4):389-398
https://doi.org/10.3349/ymj.2022.63.4.389
Yonsei Medical Journal
YMJ
pISSN: 0513-5796 · eISSN: 1976-2437

MiR-494-3p Upregulation Exacerbates Cerebral Ischemia Injury by Targeting Bhlhe40

Lingjiang Sun[1], Dandan Ji[1], Feng Zhi[1], Yu Fang[1], Zigang Zhu[1], Tong Ni[1], Qin Zhu[2], and Jie Bao[1]

[1]Department of Critical Care Medicine, Wuxi Second People's Hospital, Wuxi, Jiangsu;
[2]Department of Stomatology, Taixing Third People's Hospital, Taizhou, Jiangsu, China.

Purpose: Cerebral ischemia is related to insufficient blood supply and is characterized by abnormal reactive oxygen species (ROS) production and cell apoptosis. Previous studies have revealed a key role for basic helix-loop-helix family member e40 (Bhlhe40) in oxidative stress and cell apoptosis. This study aimed to investigate the roles of miR-494-3p in cerebral ischemia/reperfusion (I/R) injury.

Materials and Methods: A mouse middle cerebral artery occlusion (MCAO/R) model was established to mimic cerebral ischemia in vivo. Brain infarct area was assessed using triphenyl tetrazolium chloride staining. Oxygen-glucose deprivation/reoxygenation (OGD/R) operation was adopted to mimic neuronal injury in vitro. Cell apoptosis was analyzed by flow cytometry. The relationship between miR-494-3p and Bhlhe40 was validated by luciferase reporter and RNA immunoprecipitation assays.

Results: Bhlhe40 expression was downregulated both in MCAO/R animal models and OGD/R-induced SH-SY5Y cells. Bhlhe40 overexpression inhibited cell apoptosis and reduced ROS production in SH-SY5Y cells after OGD/R treatment. MiR-494-3p was verified to bind to Bhlhe40 and negatively regulate Bhlhe40 expression. Additionally, cell apoptosis and ROS production in OGD/R-treated SH-SY5Y cells were accelerated by miR-494-3p overexpression. Rescue experiments suggested that Bhlhe40 could reverse the effects of miR-494-3p overexpression on ROS production and cell apoptosis.

Conclusion: MiR-494-3p exacerbates brain injury and neuronal injury by regulating Bhlhe40 after I/R.

Key Words: Cerebral I/R injury, Bhlhe40, miR-494-3p, ROS production

INTRODUCTION

Ischemic stroke is a common nervous system disease that poses long-term disability and high rates of mortality.[1,2] Related intervention and treatment strategies seek to achieve blood flow recovery that can result in cerebral ischemia/reperfusion (I/R) injury, and accumulating reports suggest that cerebral I/R elicits an excessive release of reactive oxygen species (ROS), inflammatory responses, and cell apoptosis, leading to irreversible brain damage.[3,4] Although encouraging progress has been achieved in the field of reperfusion therapy over the last few decades,[5] therapeutic outcomes remain unsatisfactory. Hence, improved understanding of pathological mechanisms and novel treatment strategies for cerebral I/R injury are desperately needed.

Basic helix-loop-helix family member e40 (Bhlhe40), a basic helix-loop-helix protein, has been shown to play significant roles in multiple cellular behaviors, including cell differentiation, cell proliferation, cell apoptosis, and cell metabolism: Bhlhe40 has been found to mediate the inhibitory effects of hypoxia on myogenic differentiation;[6] to modulate cytokine production via T cells and be crucial for pathogenicity in autoimmune neuroinflammation;[7] and to promote cell proliferation in breast cancer.[8] Interestingly, upregulation of Bhlhe40 has been shown to decrease ROS production.[9] Nevertheless, although cerebral I/R injury is characterized by excessive ROS

Received: September 8, 2021 **Revised:** November 19, 2021
Accepted: December 21, 2021
Co-corresponding authors: Qin Zhu, MM, Department of Stomatology, Taixing Third People's Hospital, 2 Taixing West Road, Taizhou, Jiangsu 225400, China.
Tel: 86-13626134522, Fax: 86-2816222, E-mail: zhuqin0313@163.com and
Jie Bao, MM, Department of Critical Care Medicine, Wuxi Second People's Hospital, 68 Zhongshan Road, Wuxi, Jiangsu 214000, China.
Tel: 86-18851505920, Fax: 86-68562057, E-mail: baojie2280@163.com

•The authors have no potential conflicts of interest to disclose.

production, the potential role of Bhlhe40 in cerebral I/R injury has yet to be investigated.

MicroRNAs (miRNAs) are a category of short, single-stranded, noncoding RNAs (20–24 nucleotides) that are involved in numerous biological processes.[10,11] A series of miRNAs have been shown to play essential roles in pathological processes of cerebral ischemia. For example, miR-138 appears to attenuate myocardial I/R injury by inhibiting mitochondria-mediated apoptosis.[12] Researchers have also found that miR-26a is a critical mediator in exosomes derived from human urine-derived stem cells after ischemic stroke.[13] As miRNAs have previously been shown to carry out various biological functions in multiple cellular processes through complementarily binding to the 3'-untranslated region (UTR) of mRNAs,[14,15] we conducted bioinformatics analysis to predict the putative upstream miRNAs of Bhlhe40. In doing so, we determined that miR-494-3p binds to Bhlhe40: miR-494-3p inhibition was reported to prevent neurotoxic T helper cell 1-skewed neurotoxicity in a mouse model of ischemic stroke.[16] Moreover, research has indicated that miR-494-3p could contribute to neuronal network degeneration by targeting semaphorin 3A in amyotrophic lateral sclerosis.[17] Accordingly, we investigated the roles of Bhlhe40 and miR-494-3p in cerebral I/R injury using oxygen-glucose deprivation/reperfusion (OGD/R) SH-SY5Y cells and middle cerebral artery occlusion/reperfusion (MCAO/R) mice.

MATERIALS AND METHODS

Animals

Male C57BL6 mice (21–24 g, 6–8 weeks, Vital River Co. Ltd., Beijing, China) were housed under a 12 h of light/dark cycle under controlled temperature and humidity. All animal experiments were conducted in strict accordance with the Guide for the Care and Use of Laboratory Animals of the National Institutes of Health and were approved by the Experimental Animal Ethics Committee of Wuxi Second People's Hospital (Jiangsu, China).

MCAO/R operation

A mouse MCAO/R model was established as described in previous studies.[16,18] Briefly, mice were intraperitoneally injected with ketamine (65 mg/kg) and xylazine (6 mg/kg) for anesthesia. After being fixed with adhesive tape, an incision was made on the necks of mice to expose the right common carotid artery. Next, a 6–0 nylon filament with a rounded tip (Doccol Corporation, Redlands, CA, USA) was inserted from the common carotid artery into the end of the internal carotid artery to obstruct the origin of the right middle cerebral artery. Two hours after occlusion, the surgical nylon filament was removed, and reperfusion was administered for 12, 24, 48, or 72 h. Mice in the sham group were treated similarly without MCAO operation. After mice were sacrificed under deep anesthesia, brain tissues were harvested for further investigation.

SH-SY5Y cell culture

SH-SY5Y cells (Chinese Academy of Sciences, Shanghai, China) were cultured in Dulbecco's modified Eagle's medium (DMEM; Gibco-BRL, Grand Island, NY, USA) containing 10% fetal bovine serum and 1% penicillin/streptomycin (Gibco-BRL). Cells were cultured at 37°C in a humidified atmosphere with 5% CO_2.

Cell transfection

MiR-494-3p mimics, miR-494-3p inhibitor, negative control (NC) mimics, and NC inhibitor were synthesized by GenePharma (Shanghai, China). Full-length Bhlhe40 was inserted into the pcDNA3.1 vector (Invitrogen, Carlsbad, CA, USA) to generate a Bhlhe40 overexpression vector (pcDNA3.1/Bhlhe40), and an empty pcDNA3.1 vector was used as a NC. Cell transfection was performed using Lipofectamine 2000 (Invitrogen).

OGD/R operation

An OGD/R operation was adopted to mimic neuronal injury in vitro. Briefly, SH-SY5Y cells were cultured in glucose-free DMEM in a hypoxia chamber filled with N_2 (95%) and CO_2 (5%) at 37°C for 4, 8, 12, or 24 h. Subsequently, cells were cultured under normal conditions in high-glucose DMEM at 37°C for an additional 24 h.

Adeno-associated virus injection

Adeno-associated virus (AAV) (serotype 2, Vigene Biosciences, Shanghai, China) containing full-length Bhlhe40 or NC (empty AAV) was injected (10^{11} v.g/mL) into mice via the tail vein 2 weeks before MCAO/R operation.

Neurological score

Neurological deficits were determined after 24 h of MCAO/R by two investigators blinded to animal groupings. Zea-Longa score was used to score neurological deficits as follows: 0, the animal behaved normally; 1, the contralateral fore paw could not be fully extended; 2, the contralateral fore paw could not be extended; 3, animal mildly turned around in a circle to the contralateral side; 4, animal severely turned around in a circle to the contralateral side; and 5, animal fell to the contralateral side.

Triphenyl tetrazolium chloride staining

Brain infarct volume was determined using triphenyl tetrazolium chloride (TTC) staining after 24 h of MCAO/R. After mice were sacrificed, brain tissues were cut into coronal slices (2-mm thickness). The slices were stained with 1% 2,3,5-TTC (Sigma-Aldrich, St. Louis, MO, USA) at 37°C for 30 min in the dark and then fixed with 4% paraformaldehyde. The infarct area (white) and normal areas (red) were analyzed using ImageJ software (National Institutes of Health, Bethesda, MD,

https://doi.org/10.3349/ymj.2022.63.4.389

USA), and the infarct ratio was calculated by the following formula: (red area on the left-red area on the right)/red area on the left.

Quantitative real-time polymerase chain reaction

Total RNA was extracted from SH-SY5Y cells or brain tissues of mice using TRIzol reagent (Invitrogen). A TaqMan MicroRNA Reverse Transcription Kit (Applied Biosystems, Foster City, CA, USA) or High-Capacity cDNA Reverse Transcription Kit (Applied Biosystems) was used for synthesis of cDNA. U6 acted as the internal reference for miRNA expression. Real-time PCR was performed using SYBR Green Real-Time PCR MasterMix (Toyobo, Japan), with GAPDH serving as the internal reference for mRNA expression. The $2^{-\Delta\Delta Ct}$ method was used to calculate relative gene expression.

Western blot analysis

Proteins were extracted using radioimmunoprecipitation assay buffer (Cell Signaling Technology, Inc., Danvers, MA, USA). Next, the concentrations of individual proteins were determined with a Bicinchoninic Acid Protein Assay Kit (Beyotime, Beijing, China). The proteins were separated by 10% sodium dodecyl sulfate-polyacrylamide gel electrophoresis and then transferred to polyvinylidene difluoride membranes (Millipore, Billerica, MA, USA). Next, the membranes were blocked for 1 h with 5% skim milk, followed by incubation with primary antibodies at 4°C overnight. Subsequently, secondary antibody was added for another 2 h of incubation. The proteins were visualized with enhanced chemiluminescence detection kits (Beyotime) and quantified using ImageJ software. The primary antibodies included Bax (ab32503; Abcam Inc., Shanghai, China), Bcl-2 (ab182858), Bhlhe40 (ab97525), and GAPDH (ab181602).

Flow cytometry analysis

The apoptosis rate of SH-SY5Y cells was examined with flow cytometry with an Annexin V-FITC/PI Detection Kit (Beyotime). The cell suspension was digested in trypsin, washed with phosphate buffer saline, and then centrifuged for 10 min. After being resuspended in binding buffer, SH-SY5Y cells were incubated with Annexin V-FITC (5 μL) and propidium iodide (5 μL) for 15 min at room temperature in the dark. A FC500MCL flow cytometer (BD Biosciences, San Jose, CA, USA) was used to assess apoptosis.

Bioinformatics analysis

The online database starBase (http://starbase.sysu.edu.cn/) was used to predict the miRNAs that have binding sites for Bhlhe40. The binding site of miR-494-3p in Bhlhe40 was predicted in the TargetScan database (http://www.targetscan.org/vert_70/).

Dual-luciferase reporter assay

The 3'-UTR of Bhlhe40 was inserted into the pmirGLO reporter vector (Promega, Madison, WI, USA) to construct a wild-type Bhlhe40-expressing vector (Bhlhe40-Wt). Site-specific mutagenesis of *TSPAN5* was performed to generate mutant (Mut) TSPAN5 (Bhlhe40-Mut). Then, Bhlhe40-Wt or Bhlhe40-Mut vectors were co-transfected, respectively, with NC-mimics, miR-494-3p mimics, NC-inhibitor, or miR-494-3p inhibitor into cells. Lipofectamine 2000 (Invitrogen) was used for transfection. After 48 h of transfection, luciferase activity was determined using a dual-luciferase assay system (Promega).

RNA immunoprecipitation assay

RNA immunoprecipitation (RIP) assay was conducted using an EZ-Magna RIP Kit (Millipore) following the manufacturer's instructions. Briefly, prepared magnetic beads coated with anti-Ago2 and the NC anti-IgG were added to cell lysates for incubation at 4°C overnight. RIP wash buffer was added to wash the beads. After purification with proteinase K, the purified RNA contents were subjected to RT-PCR.

Measurement of ROS

In order to measure the production of ROS, SH-SY5Y cells were cultured in DMEM supplemented with 0.1% 2',7'-dichlorodihydrofluorescein diacetate for 30 min at 37°C according to the protocols of an ROS Assay Kit (Beyotime). Cells were then collected by centrifugation and resuspended in phosphate buffer saline. Fluorescence intensity was determined using a Microplate Reader (Molecular Devices, Sunnyvale, CA, USA) at an optimal excitation wavelength of 500 nm and an emission wavelength of 525 nm.

Statistical analysis

Data are expressed as the means±standard deviation from three independent experiments and were analyzed using SPSS 23.0 (IBM Corp., Armonk, NY, USA). Student's t-test or one-way analysis of variance (ANOVA) followed by Tukey's post hoc test was used for comparisons between groups. *P* values <0.05 were considered statistically significant.

RESULTS

Bhlhe40 alleviates cerebral I/R injury in a MCAO/R animal model

We performed Western blotting to examine Bhlhe40 levels in a MCAO/R mouse model. The results showed that Bhlhe40 protein levels were reduced after MCAO/R in a time-dependent manner after a minimum of 48 h ($p<0.01$, ANOVA followed by Tukey's post hoc test) (Fig. 1A and B). Next, we explored the effects of Bhlhe40 on mice after MCAO/R. First, Bhlhe40 was upregulated in the animal model by injection with AAV-Bhlhe40 ($p<0.001$, ANOVA followed by Tukey's post hoc test) (Fig. 1C). In order to evaluate brain infarct volumes in mice, TTC staining was performed after 48 h of reperfusion. We found

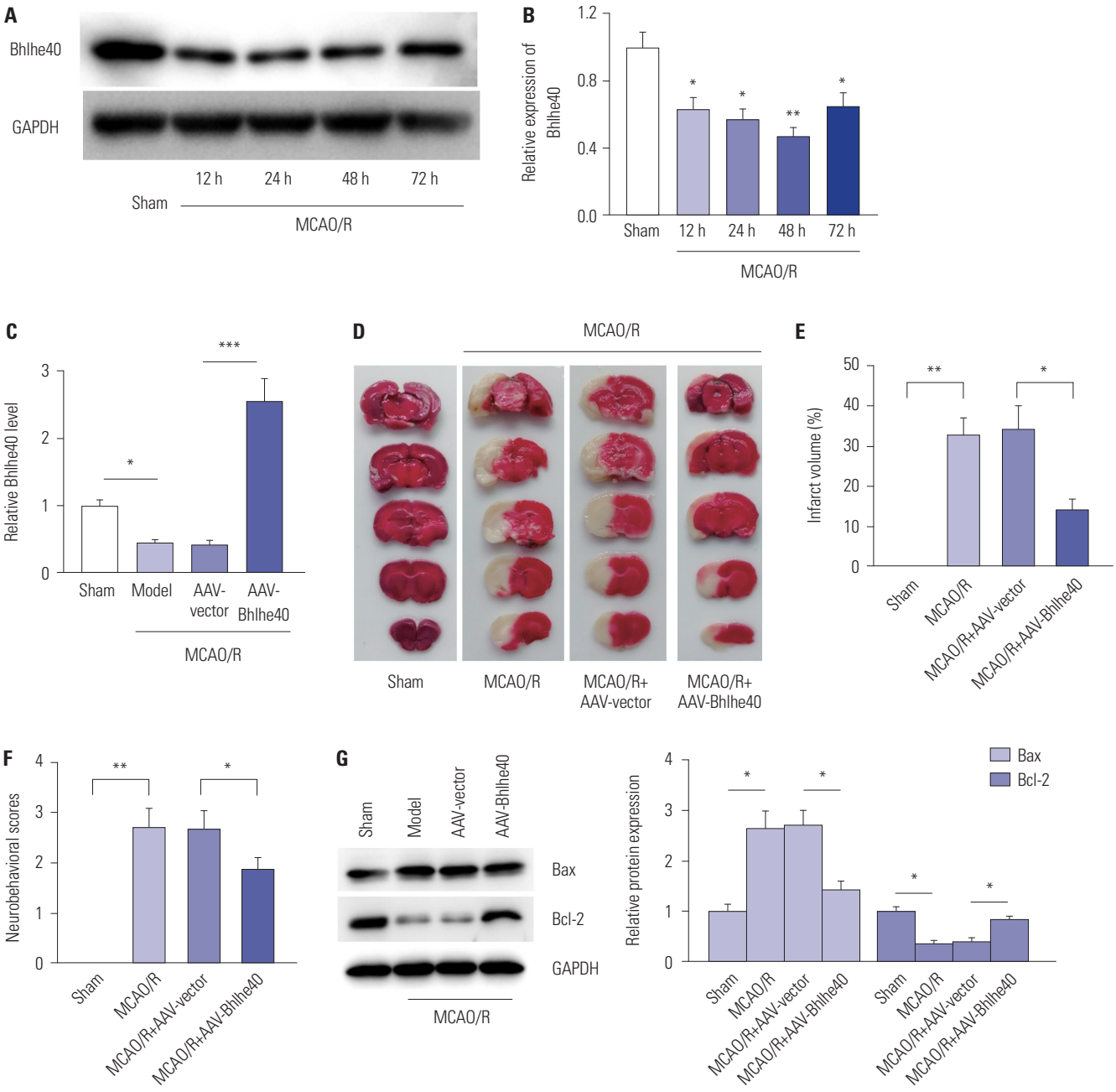

Fig. 1. Bhlhe40 alleviates cerebral I/R injury in a MCAO/R animal model. (A and B) Bhlhe40 protein levels in brain tissues of mice (n=8/group) were measured by Western blot after MCAO/R treatment for 12, 24, 48, or 72 h. *p<0.05, **p<0.01, ANOVA followed by Tukey's post hoc test. (C) Bhlhe40 expression in brain tissues of mice (n=8/group) was measured by RT-qPCR after injection with AAV-Bhlhe40. *p<0.05, ***p<0.001, ANOVA followed by Tukey's post hoc test. (D and E) TTC staining results of the cerebral cortex in mice (n=8/group) at 48 h after MCAO/R. *p<0.05, **p<0.01, ANOVA followed by Tukey's post hoc test. (F) Measurements of neurological scores in mice (n=8/group). *p<0.05, **p<0.01, ANOVA followed by Tukey's post hoc test. (G) Western blot analysis was performed to determine Bax and Bcl-2 protein expression in brain tissues of mice (n=8/group). *p<0.05, ANOVA followed by Tukey's post hoc test. I/R, schemia/reperfusion; MCAO/R, middle cerebral artery occlusion; Bhlhe40, basic helix-loop-helix family member e40; ANOVA, analysis of variance; AAV, adeno-associated virus; TTC, triphenyl tetrazolium chloride.

that infarct volume was significantly increased in the MCAO/R group, compared with the sham group (p<0.01, ANOVA followed by Tukey's post hoc test), while Bhlhe40 overexpression reduced the infarct volume, compared with the model group (p<0.05, ANOVA followed by Tukey's post hoc test) (Fig. 1D and E). Moreover, we observed that neurological scores notably decreased after overexpressing Bhlhe40 in the MCAO/R group (p<0.05, ANOVA followed by Tukey's post hoc test) (Fig. 1F). Western blot analysis indicated that Bhlhe40 overexpression decreased the expression of Bax and increased that of Bcl-2 in MCAO/R mice (p<0.05, ANOVA followed by Tukey's post hoc test) (Fig. 1G).

https://doi.org/10.3349/ymj.2022.63.4.389

Bhlhe40 inhibits cell apoptosis and ROS production in OGD/R-induced SH-SY5Y cells

We found that the Bhlhe40 protein levels in SH-SY5Y cells were gradually reduced after OGD/R treatment at 4, 8, 12, and 24 h (p<0.01, ANOVA followed by Tukey's post hoc test) (Fig. 2A and B). Bhlhe40 was overexpressed with pcDNA3.1/Bhlhe40 transfection in OGD/R-treated SH-SY5Y cells (p<0.001, ANOVA followed by Tukey's post hoc test) (Fig. 2C). Western blot revealed that Bax protein expression was increased and that Bcl-2 protein expression was reduced in the OGD/R group; however, Bhlhe overexpression reversed these changes (p<0.05, ANOVA followed by Tukey's post hoc test) (Fig. 2D). Flow cytometry analysis demonstrated that the cell apoptosis rate in OGD/R-treated SH-SY5Y cells was decreased after overexpressing Bhlhe40 (p<0.05, ANOVA followed by Tukey's post hoc test) (Fig. 2E). Furthermore, we discovered that the production of ROS was inhibited after Bhlhe40 overexpression (p<0.05, ANOVA followed by Tukey's post hoc test) (Fig. 2F).

MiR-494-3p targets Bhlhe40

We searched the starBase v3.0 database to identify miRNAs with binding sites to Bhlhe40, and six candidate miRNAs were identified (Fig. 3A) (condition: the overlapped gene in human and mouse). The miRNAs are listed in Supplementary Tables 1 and 2 (only online). In response to OGD/R treatment, miR-494-3p levels significantly increased, while the other miRNAs displayed no significant change (p<0.01, Student's t-test) (Fig. 3B). In addition, miR-494-3p was present at higher levels in the MCAO/R group than in the sham group (p<0.05, Student's t-test) (Fig. 3C). Next, miR-494-3p levels were upregulated by transfection with miR-494-3p mimics and downregulated by miR-494-3p inhibitor (p<0.001, ANOVA followed by Tukey's post hoc test) (Fig. 3D). We found that Bhlhe40 expression was decreased in SH-SY5Y cells in the miR-494-3p mimics group and increased in the miR-494-3p inhibitor group (p<0.01, ANOVA followed by Tukey's post hoc test) (Fig. 3E). After RIP assay, Bhlhe40 and miR-494-3p were found to be significantly enriched in the anti-Ago2 group, compared with the anti-IgG group (p<0.001, ANOVA followed by Tukey's post hoc test) (Fig. 3F). Furthermore, luciferase reporter assay results showed that the luciferase activity of Bhlhe40-Wt was markedly reduced by miR-494-3p mimics and increased by miR-494-3p inhibitor, compared with the control group. The luciferase activity of Bhlhe40-Mut exhibited no significant change among SH-SY5Y cells in the NC-mimics, miR-494-3p mimics, NC-inhibitor, and miR-494-3p inhibitor groups (p<0.01, ANOVA followed by Tukey's post hoc test) (Fig. 3G), suggesting that Bhlhe40 is targeted by miR-494-3p.

Overexpression of miR-494-3p promotes ROS production and neuron apoptosis

In order to further explore the biological function of miR-494-3p, RT-qPCR was performed, and the expression of miR-494-3p in OGD/R-treated SH-SY5Y cells was upregulated by transfection with miR-494-3p mimics and downregulated by transfection with miR-494-3p inhibitor (p<0.001, ANOVA followed by Tukey's post hoc test) (Fig. 4A). Overexpressing miR-494-3p increased apoptosis, while knockdown of miR-494-3p prevented cells from apoptosis in the OGD/R group (p<0.05, ANOVA followed by Tukey's post hoc test) (Fig. 4B). As shown in Fig. 4C, in response to miR-494-3p mimics, Bax protein levels were increased, and Bcl-2 protein levels were decreased. In the miR-494-3p inhibitor group, Bax protein levels were decreased, and Bcl-2 protein levels were increased (p<0.05, ANOVA followed by Tukey's post hoc test). Moreover, miR-494-3p overexpression reduced ROS production, while miR-494-3p downregulation had the opposite effect (p<0.05, ANOVA followed by Tukey's post hoc test) (Fig. 4D).

Bhlhe40 can rescue the effects of miR-494-3p on neuron apoptosis and ROS production

Finally, rescue assays were conducted to determine whether Bhlhe40 improves I/R by interacting with miR-494-3p. The results showed that miR-494-3p mimics increased cell apoptosis and Bax protein expression and the decreased Bcl-2 protein level, while Bhlhe40 overexpression could counteract these effects (p<0.05, ANOVA followed by Tukey's post hoc test) (Fig. 5A and B). Additionally, overexpression of Bhlhe40 attenuated the promotive role of miR-494-3p in ROS production (p<0.05, ANOVA followed by Tukey's post hoc test) (Fig. 5C). Therefore, miR-494-3p was deemed to promote cell apoptosis and ROS production by targeting Bhlhe40.

DISCUSSION

Bhlhe40 influences cell apoptosis and oxidative stress, and ROS production could be decreased by Bhlhe40 upregulation.[9] The present study was the first to demonstrate that the expression of Bhlhe40 is downregulated in brain tissues of MCAO/R mice and OGD/R-induced SH-SY5Y cells. Next, we further explored the role of Bhlhe40 in cerebral I/R injury. After a series of experiments, Bhlhe40 overexpression was found to reduce brain infract volume and neurobehavioral scores in MCAO/R animal models. Similarly, Bhlhe40 overexpression restrained cell apoptosis and ROS production in OGD/R-induced SH-SY5Y cells, suggesting the protective effects of Bhlhe40 against cerebral I/R injury.

Cerebral I/R injury is considered a destructive brain process. Unfortunately, clinical treatment of I/R induced brain injury remains limited. Meanwhile, research has shown ROS to play an important role in the pathological process of cerebral I/R injury.[19,20] Reportedly, a significantly increase of ROS in cerebral I/R injury leads to oxidative stress and evokes multiple pro-apoptotic signaling pathways:[21-23] For example, dihydrocapsaicin restrains oxidative stress and inflammatory responses

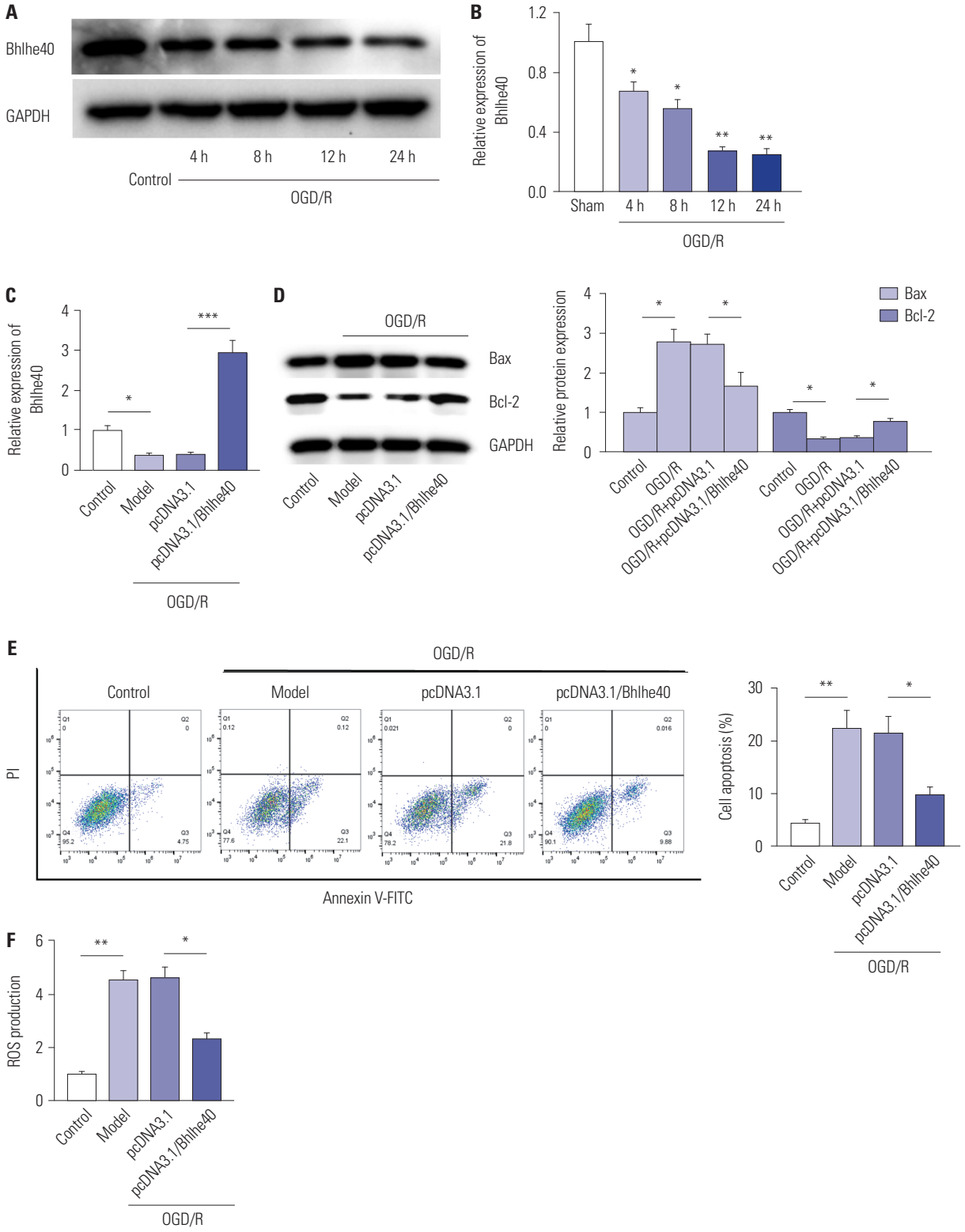

Fig. 2. Bhlhe40 inhibits cell apoptosis and ROS production in OGD/R-induced SH-SY5Y cells. (A and B) Bhlhe40 protein levels in SH-SY5Y cells were measured by Western blot after OGD/R treatment for 4, 8, 12, or 24 h. *p<0.05, **p<0.01, ANOVA followed by Tukey's post hoc test. (C) The transfection efficiency of pcDNA3.1/Bhlhe40 in OGD/R-treated SH-SY5Y cells was determined by RT-qPCR. *p<0.05, ***p<0.001, ANOVA followed by Tukey's post hoc test. (D) Bax and Bcl-2 protein expression levels were detected by Western blot. *p<0.05, ANOVA followed by Tukey's post hoc test. (E) Flow cytometry was used to determine apoptosis in OGD/R-treated SH-SY5Y cells. *p<0.05, **p<0.01, ANOVA followed by Tukey's post hoc test. (F) ROS production in OGD/R-treated SH-SY5Y cells. *p<0.05, **p<0.01, ANOVA followed by Tukey's post hoc test. Bhlhe40, basic helix-loop-helix family member e40; ROS, reactive oxygen species; OGD/R, oxygen-glucose deprivation/reoxygenation; ANOVA, analysis of variance.

https://doi.org/10.3349/ymj.2022.63.4.389

through inhibiting the release of ROS.[24] Additionally, pretreatment of melatonin was found to diminish increased expression levels of Nox2 and Nox4 and thereby reduce the ROS levels in cerebral I/R.[25] Progranulin (PGRN) is a secreted glycoprotein with pleiotropic functions and it protects against cerebral I/R-induced brain injury by suppressing necroptosis and associated ROS production.[26]

MiRNAs have been widely reported to participate in multiple biological processes.[10,11] Some miRNAs have been shown to play roles in ischemic injury.[12,13] After a series of assays, we verified

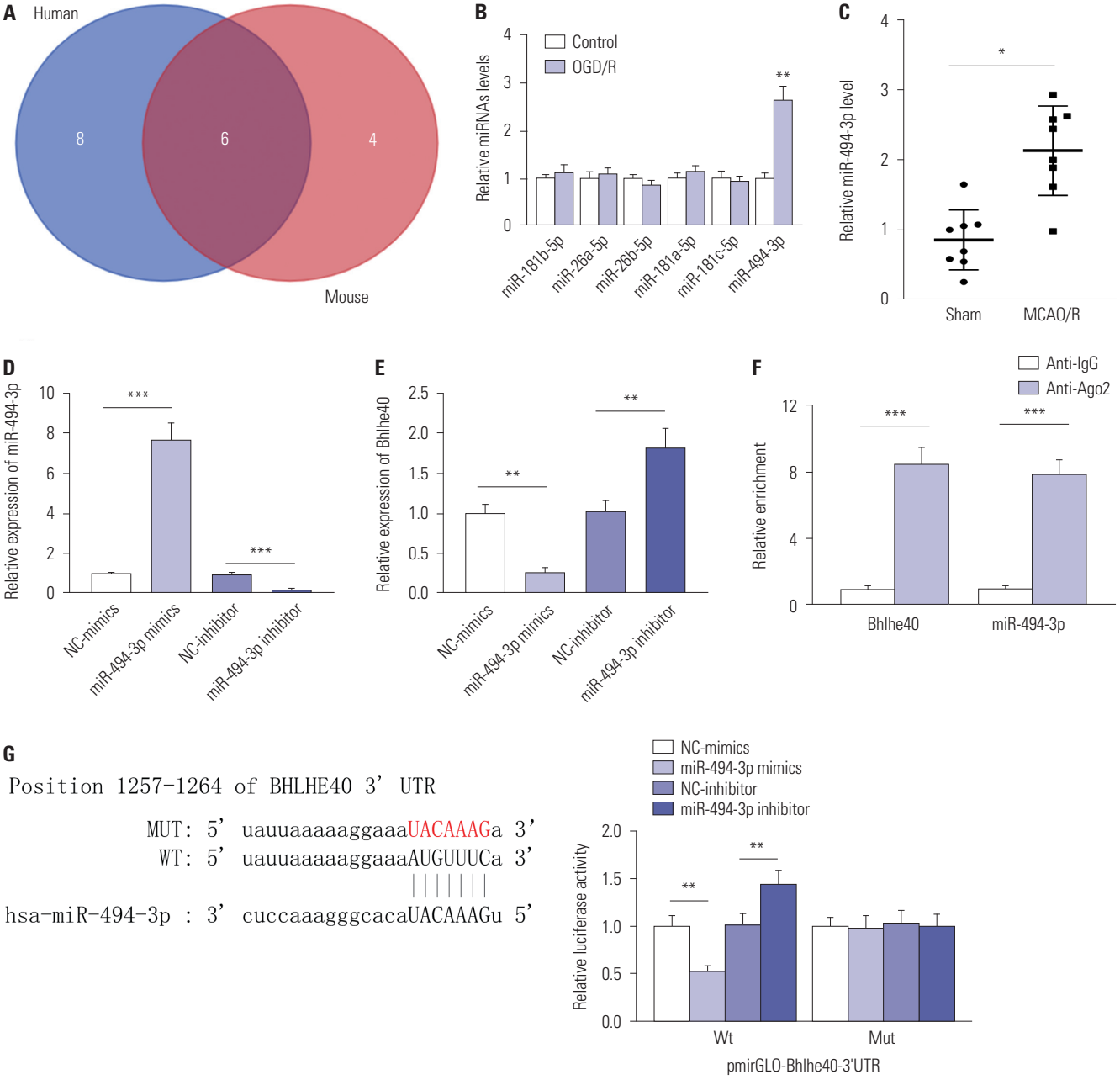

Fig. 3. MiR-494-3p directly interacts with Bhlhe40. (A) Venn diagram showing the predicted miRNAs that have binding sites for Bhlhe40. (B) The expression levels of miR-181b-5p, miR-26a-5p, miR-26b-5p, miR-181a-5p, and miR-494-3p in SH-SY5Y cells were measured by RT-qPCR. $^{**}p<0.01$, Student's t-test. (C) The levels of miR-494-3p in brain tissues of mice (n=8/group) was determined by RT-qPCR. $^{*}p<0.05$, Student's t-test. (D) The overexpression and knockdown efficiency of miR-494-3p mimics and miR-494-3p inhibitor were determined by RT-qPCR, respectively. $^{***}p<0.001$, ANOVA followed by Tukey's post hoc test. (E) Bhlhe40 levels in the context of miR-494-3p overexpression or inhibition were examined by RT-qPCR. $^{**}p<0.01$, ANOVA followed by Tukey's post hoc test. (F) RIP and RT-qPCR assays for the enrichment of miR-494-3p and Bhlhe40 in IgG or Ago2 group. $^{***}p<0.001$, ANOVA followed by Tukey's post hoc test. (G) Bhlhe40-Wt or Bhlhe40-Mut vectors were co-transfected with miR-494-3p mimics, NC-mimics, miR-494-3p inhibitor, or NC-inhibitor into SH-SY5Y cells. The luciferase activity of Bhlhe40-Wt or Bhlhe40-Mut vector was detected by dual luciferase reporter assay. $^{**}p<0.01$, ANOVA followed by Tukey's post hoc test. Bhlhe40, basic helix-loop-helix family member e40; ANOVA, analysis of variance; RIP, RNA immunoprecipitation; NC, negative control; OGD/R, oxygen-glucose deprivation/reoxygenation; MCAO/R, middle cerebral artery occlusion.

that Bhlhe40 could bind to miR-494-3p. Previously, miR-494-3p was reported to aggravate 1-methyl-4-phenylpyridinium-induced neurotoxicity.[27] Additionally, miR-494-3p could serve as a potential biomarker or a therapeutic target for stroke induced by atrial fibrillation.[28] Its functional and potential mechanisms in cerebral I/R injury are still unclear. In our research, miR-494-3p upregulation accelerated cell apoptosis and ROS production in OGD/R-induced SH-SY5Y cells, and miR-494-3p downregulation inhibited cell apoptosis and ROS production. Interestingly, Bhlhe40 overexpression reversed the influence of miR-

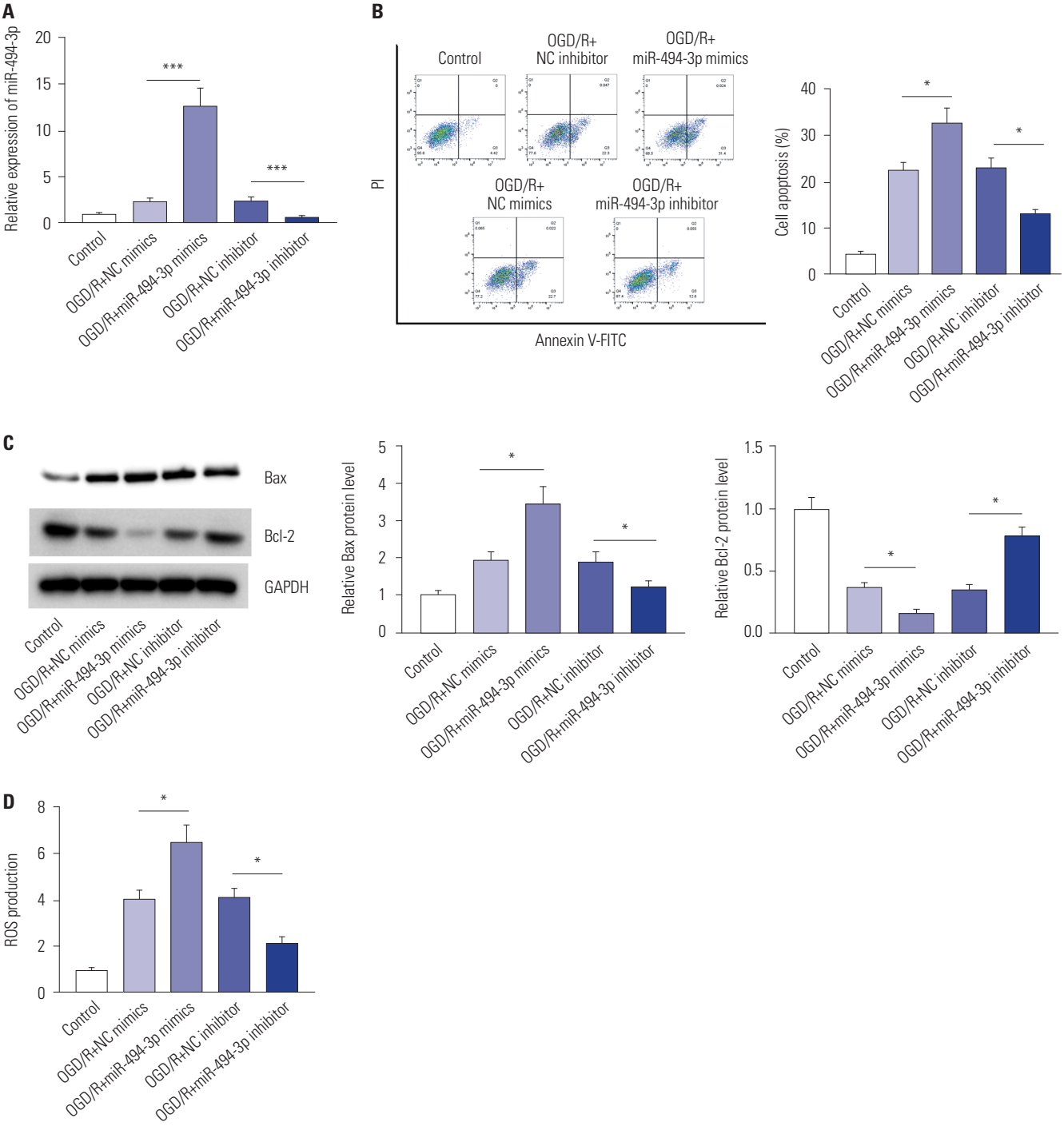

Fig. 4. Overexpression of miR-494-3p aggravates I/R injury. (A) The transfection efficiency of miR-494-3p mimics or miR-494-3p inhibitor in OGD/R-treated SH-SY5Y cells was determined by RT-qPCR. ***p<0.001, ANOVA followed by Tukey's post hoc test. (B) Flow cytometry analysis was used to detect cell apoptosis in the indicated groups. *p<0.05, ANOVA followed by Tukey's post hoc test. (C) Western blot was conducted to measure Bax and Bcl-2 protein expression levels in the indicated groups. *p<0.05, ANOVA followed by Tukey's post hoc test. (D) ROS production in the indicated groups. *p<0.05, ANOVA followed by Tukey's post hoc test. I/R, schemia/reperfusion; OGD/R, oxygen-glucose deprivation/reoxygenation; ANOVA, analysis of variance; ROS, reactive oxygen species; NC, negative control.

https://doi.org/10.3349/ymj.2022.63.4.389

494-3p overexpression on cell apoptosis and ROS production in OGD/R-induced SH-SY5Y cells.

In summary, this study is the first to demonstrate a protective role for Bhlhe40 against cerebral I/R injury in vitro and in vivo. Additionally, we found that miR-494-3p promotes cell apoptosis and ROS production in OGD/R-induced SH-SY5Y cells at least partly by targeting Bhlhe40. Our findings indicate that a miR-494-3p/Bhlhe40 axis may be a promising therapeu-

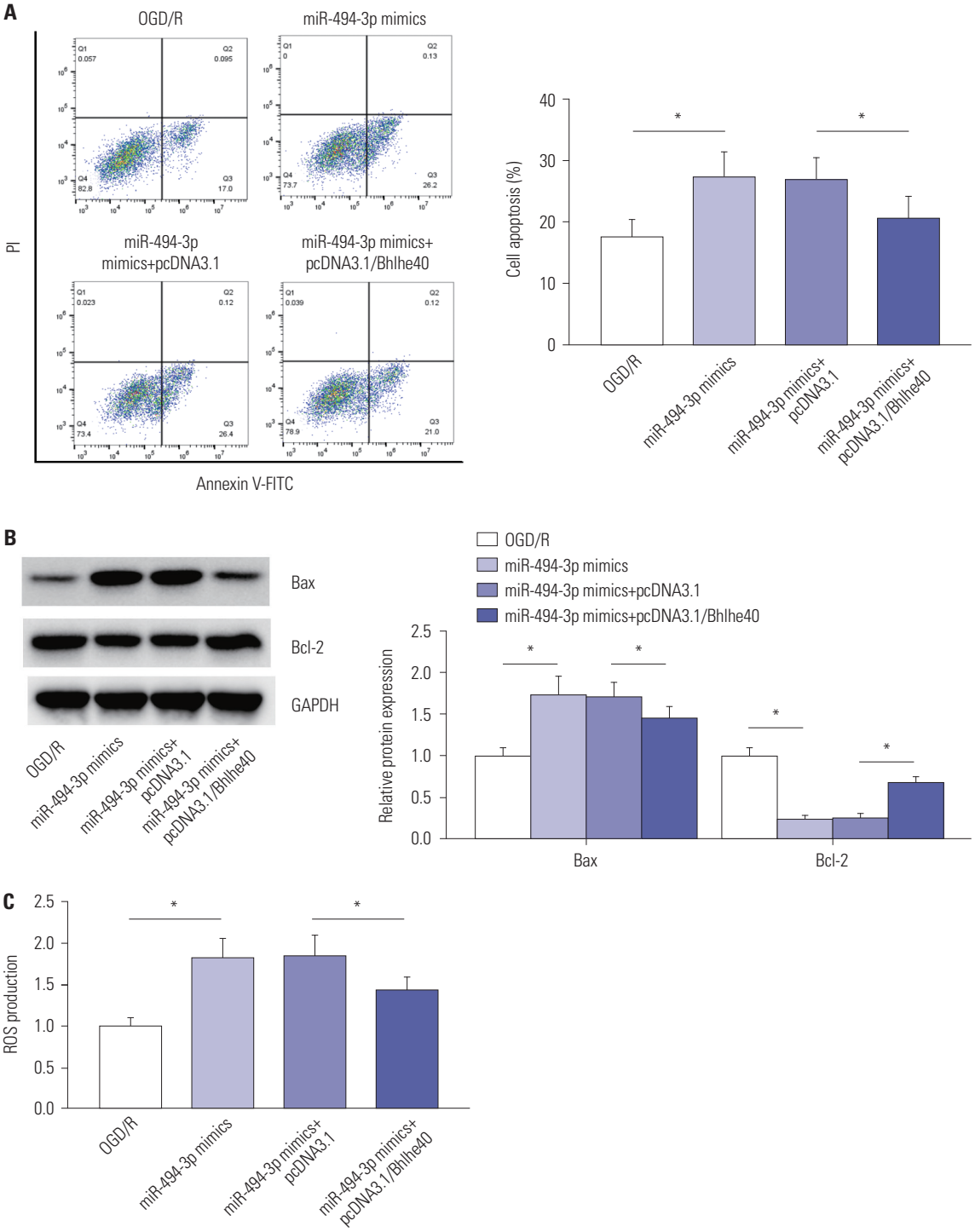

Fig. 5. Bhlhe40 rescues the effects of miR-494-3p on OGD/R-induced apoptosis and ROS production. (A) Flow cytometry was used to assess apoptosis in OGD/R SH-SY5Y cells transfected with the indicated plasmids. *p<0.05, ANOVA followed by Tukey's post hoc test. (B) Bax and Bcl-2 protein expression levels in OGD/R SH-SY5Y cells transfected with the indicated plasmids were measured by Western blot. *p<0.05, ANOVA followed by Tukey's post hoc test. (C) ROS production in OGD/R SH-SY5Y cells transfected with the indicated plasmids. *p<0.05, ANOVA followed by Tukey's post hoc test. Bhlhe40, basic helix-loop-helix family member e40; OGD/R, oxygen-glucose deprivation/reoxygenation; ROS, reactive oxygen species; ANOVA, analysis of variance.

tic target for cerebral I/R injury and may provide a scientific basis for targeted treatment for this disease.

ACKNOWLEDGEMENTS

We appreciate the help of all participants in this study.

AUTHOR CONTRIBUTIONS

Conceptualization: Lingjiang Sun and Jie Bao. Data curation: Feng Zhi, Qin Zhu, and Zigang Zhu. Formal analysis: Dandan Ji. Funding acquisition: Lingjiang Sun. Investigation: Tong Ni, Qin Zhu, and Zigang Zhu. Methodology: Lingjiang Sun. Project administration: Lingjiang Sun, Qin Zhu, and Dandan Ji. Resources: Jie Bao. Software: Yu Fang. Supervision: Dandan Ji. Validation: Feng Zhi and Yu Fang. Visualization: Feng Zhi and Tong Ni. Writing—original draft: Lingjiang Sun. Writing—review & editing: Lingjiang Sun and Jie Bao. Approval of final manuscript: all authors.

ORCID iDs

Lingjiang Sun	https://orcid.org/0000-0002-7000-2007
Dandan Ji	https://orcid.org/0000-0003-1805-7171
Feng Zhi	https://orcid.org/0000-0003-3615-6392
Yu Fang	https://orcid.org/0000-0003-4215-1870
Zigang Zhu	https://orcid.org/0000-0002-3776-8625
Tong Ni	https://orcid.org/0000-0002-4878-4268
Qin Zhu	https://orcid.org/0000-0003-1991-8375
Jie Bao	https://orcid.org/0000-0003-3870-8138

REFERENCES

1. Ghosh MK, Chakraborty D, Sarkar S, Bhowmik A, Basu M. The interrelationship between cerebral ischemic stroke and glioma: a comprehensive study of recent reports. Signal Transduct Target Ther 2019;4:42.
2. Goldstein LB, Adams R, Becker K, Furberg CD, Gorelick PB, Hademenos G, et al. Primary prevention of ischemic stroke: a statement for healthcare professionals from the Stroke Council of the American Heart Association. Stroke 2001;32:280-99.
3. Schrepfer E, Scorrano L. Mitofusins, from mitochondria to metabolism. Mol Cell 2016;61:683-94.
4. Rønning OM. Reperfusion therapy in stroke cases with unknown onset. Tidsskr Nor Laegeforen 2016;136:1333.
5. Shi L, Rocha M, Leak RK, Zhao J, Bhatia TN, Mu H, et al. A new era for stroke therapy: integrating neurovascular protection with optimal reperfusion. J Cereb Blood Flow Metab 2018;38:2073-91.
6. Wang C, Liu W, Liu Z, Chen L, Liu X, Kuang S. Hypoxia inhibits myogenic differentiation through p53 protein-dependent induction of Bhlhe40 protein. J Biol Chem 2015;290:29707-16.
7. Lin CC, Bradstreet TR, Schwarzkopf EA, Sim J, Carrero JA, Chou C, et al. Bhlhe40 controls cytokine production by T cells and is essential for pathogenicity in autoimmune neuroinflammation. Nat Commun 2014;5:3551.
8. Liu R, Tang A, Wang X, Chen X, Zhao L, Xiao Z, et al. Inhibition of lncRNA NEAT1 suppresses the inflammatory response in IBD by modulating the intestinal epithelial barrier and by exosome-mediated polarization of macrophages. Int J Mol Med 2018;42:2903-13.
9. Chang HC, Kao CH, Chung SY, Chen WC, Aninda LP, Chen YH, et al. Bhlhe40 differentially regulates the function and number of peroxisomes and mitochondria in myogenic cells. Redox Biol 2019;20:321-33.
10. Tyagi S, Sharma S, Ganie SA, Tahir M, Mir RR, Pandey R. Plant microRNAs: biogenesis, gene silencing, web-based analysis tools and their use as molecular markers. 3 Biotech 2019;9:413.
11. Luo X, Wang J, Wei X, Wang S, Wang A. Knockdown of lncRNA MFI2-AS1 inhibits lipopolysaccharide-induced osteoarthritis progression by miR-130a-3p/TCF4. Life Sci 2020;240:117019.
12. Liu Y, Zou J, Liu X, Zhang Q. MicroRNA-138 attenuates myocardial ischemia reperfusion injury through inhibiting mitochondria-mediated apoptosis by targeting HIF1-α. Exp Ther Med 2019;18:3325-32.
13. Ling X, Zhang G, Xia Y, Zhu Q, Zhang J, Li Q, et al. Exosomes from human urine-derived stem cells enhanced neurogenesis via miR-26a/HDAC6 axis after ischaemic stroke. J Cell Mol Med 2020;24:640-54.
14. Zhao M, Chen N, Li X, Lin L, Chen X. MiR-19a modulates hypoxia-mediated cell proliferation and migration via repressing PTEN in human pulmonary arterial smooth muscle. Life Sci 2019;239:116928.
15. Yuan X, Pan J, Wen L, Gong B, Li J, Gao H, et al. MiR-590-3p regulates proliferation, migration and collagen synthesis of cardiac fibroblast by targeting ZEB1. J Cell Mol Med 2020;24:227-37.
16. Zhao H, Li G, Wang R, Tao Z, Ma Q, Zhang S, et al. Silencing of microRNA-494 inhibits the neurotoxic Th1 shift via regulating HDAC2-STAT4 cascade in ischaemic stroke. Br J Pharmacol 2020;177:128-44.
17. Varcianna A, Myszczynska MA, Castelli LM, O'Neill B, Kim Y, Talbot J, et al. Micro-RNAs secreted through astrocyte-derived extracellular vesicles cause neuronal network degeneration in C9orf72 ALS. EBioMedicine 2019;40:626-35.
18. Trotman-Lucas M, Kelly ME, Janus J, Gibson CL. Middle cerebral artery occlusion allowing reperfusion via common carotid artery repair in mice. J Vis Exp 2019;143:e58191.
19. Lin LS, Wang JF, Song J, Liu Y, Zhu G, Dai Y, et al. Cooperation of endogenous and exogenous reactive oxygen species induced by zinc peroxide nanoparticles to enhance oxidative stress-based cancer therapy. Theranostics 2019;9:7200-9.
20. Heusch G, Schulz R. A radical view on the contractile machinery in human heart failure. J Am Coll Cardiol 2011;57:310-2.
21. Xu FF, Zhang ZB, Wang YY, Wang TH. Brain-derived glia maturation factor β participates in lung injury induced by acute cerebral ischemia by increasing ROS in endothelial cells. Neurosci Bull 2018;34:1077-90.
22. Tang Y, Shen J, Zhang F, Yang FY, Liu M. Human serum albumin attenuates global cerebral ischemia/reperfusion-induced brain injury in a Wnt/β-Catenin/ROS signaling-dependent manner in rats. Biomed Pharmacother 2019;115:108871.
23. Zhao Y, Yan F, Yin J, Pan R, Shi W, Qi Z, et al. Synergistic interaction between zinc and reactive oxygen species amplifies ischemic brain injury in rats. Stroke 2018;49:2200-10.
24. Janyou A, Wicha P, Jittiwat J, Suksamrarn A, Tocharus C, Tocharus J. Dihydrocapsaicin attenuates blood brain barrier and cerebral damage in focal cerebral ischemia/reperfusion via oxidative stress and inflammatory. Sci Rep 2017;7:10556.
25. Li H, Wang Y, Feng D, Liu Y, Xu M, Gao A, et al. Alterations in the time course of expression of the Nox family in the brain in a rat experimental cerebral ischemia and reperfusion model: effects of melatonin. J Pineal Res 2014;57:110-9.
26. Li Y, Wang YW, Chen X, Ma RR, Guo XY, Liu HT, et al. MicroRNA-4472 promotes tumor proliferation and aggressiveness in breast cancer by targeting RGMA and inducing EMT. Clin Breast Cancer 2020;20:e113-26.
27. Deng C, Zhu J, Yuan J, Xiang Y, Dai L. Pramipexole inhibits MPP+-induced neurotoxicity by miR-494-3p/BDNF. Neurochem Res 2020;45:268-77.
28. Zou R, Zhang D, Lv L, Shi W, Song Z, Yi B, et al. Bioinformatic gene analysis for potential biomarkers and therapeutic targets of atrial fibrillation-related stroke. J Transl Med 2019;17:45.